Utilizing Antiguided Structures in VCSEL-Based 2-D Active Photonic Lattices Enables Single-Mode Operation with Larger Apertures

By Luke J. Mawst

Coupled vertical cavity surface-emitting laser (VCSEL) arrays are an attractive means to increase the coherent output power of VCSELs. Single-mode VCSELs, with output powers greater than 10 mW, would be useful as telecommunication transmitters (λ=1.3-1.55 μm) or sources for optical interconnects. Commercially available single-mode VCSELs, even at shorter wavelengths (λ=0.85 μm), are generally limited to a few milliwatts of output power. The conventional VCSEL structure incorporates a built-in positive-index waveguide, designed to support a single fundamental mode. Promising results in the 3-5 mW range (λ=0.85 μm) have been obtained from wet-oxidized, positive-index-guided VCSELs [1], [2] with small emission apertures (less than 3.5 μm-dia). The small aperture size leads to a high electrical resistance and high current density, which can impact device reliability.

A larger emitting aperture is essential to reduce thermal rollover and achieve higher output powers with reliable operation. However, poor intermodal discrimination, gain-spatial-hole burning, and thermally induced self-focusing prevent single-mode outputs from larger aperture devices. Furthermore, to minimize nonlinear above-threshold effects, a relatively large built-in index step is desirable for mode stability in active devices. Unfortunately, positive-index-guided structures posses an inherent tradeoff between aperture size and index step, due to the modal cutoff conditions for single-mode operation.

By contrast, antiguided VCSEL structures have shown promise for achieving larger aperture single-mode operation. To obtain high single-mode powers with a larger emitting aperture, the use of a negative-index guide (antiguide) is beneficial.

8755-3996/03/$17.00 ©2003 IEEE

Antiguides have demonstrated high-power, single-mode operation from edge-emitting lasers [3] and, more recently, have been implemented in VCSELs [4]-[6]. This article discusses antiguided structures and some of their advantages when incorporated in 2-D VCSEL array structures.

Antiguided Structures

Antiguided structures offer some unique advantages for spatial-mode control in semiconductor diode lasers: 1) large built-in refractive index step ($\Delta n > 0.05$) for mode stability against thermal- and carrier-induced index variations, 2) strong high-order mode discrimination based on edge radiation losses, and 3) parallel coupling for high spatial coherence and stability against coupling-induced instabilities [7]. These properties have been experimentally verified, demonstrating single-mode CW output powers in the 0.5 W range from resonant optical waveguide (ROW) phase-locked arrays [8].

An antiguide consists of a low-index core region, clad by high-index regions [Figure 1(a)]. An optical mode can exist in such a structure provided sufficient gain is introduced into the low-index core to compensate for the loss due to refraction into the high-index cladding layers. By contrast with a positive-index guide, an antiguide can propagate a single-mode even in a large index-step structure, since high-order modes suffer excessively large edge radiation. This property of possessing a large index step with strong mode discrimination makes the antiguide a natural choice for the semiconductor diode laser waveguide. Unfortunately, a single antiguide can have excessively high edge losses (α=50-100 cm^{-1}), even for the fundamental mode. To make practical use of the antiguide for diode laser mode control, two different structures have been developed to lower the loss of the fundamental mode while maintaining the advantages of the antiguide: 1) the ROW array [7] and 2) the antiresonant reflecting optical waveguide (ARROW) structure [9]. These two techniques have been successfully demonstrated in edge-emitting diode lasers, resulting in watt-range spatially coherent power levels.

In an antiguided array structure [Figure 1(b)], leaked radiation from each antiguide element (low-index region) optically couples neighboring elements to phase lock the structure as well as lower the total edge radiation loss to an acceptable level. If an additional lateral resonance requirement is met, which is that each interelement region corresponds to an integral number of lateral half-waves ($\lambda_1/2$, see Figure 1), then the leaked radiation is fully transmitted throughout the entire structure resulting in parallel coupling [7]. This so-called ROW array provides strong mode discrimination, allowing the structure to oscillate only in the resonant mode with mode stability demonstrated to high-output power levels. Large aperture, Al-free, nearly resonant arrays with 200 µm-wide (40 elements) emitting apertures have recently demonstrated 10 W pulsed power with a beam width of only 2x diffraction limit[10].

Antiguided VCSELs have been realized either by surrounding a low-index core region by regrowth of a high-index material [4] or by creating a low-index core region by shifting the cavity resonance (towards longer wavelength) outside the core [5], [6]. The latter structure relies on the cavity-induced index-step proposed by Hadley [11]. These devices display promising results; single-mode operation up to 5-15 $\times I_{th}$ for diameters as large as 16 µm wide have been achieved [4]-[6]. On the other hand, the power has been limited to less than 2 mW because of the relatively large radiation loss incurred for the fundamental mode, which is inherent to the antiguide structure [12]. One attractive approach to reduce the edge losses of the antiguide while maintaining mode selectivity is to form a coupled 2-D VCSEL array using antiguides as the array elements. In this way, the radiation leakage from each antiguide optically couples other elements of the array, creating a large-area VCSEL with high spatial coherence.

Active Photonic Lattices

Photonic-lattice structures in the near-IR wavelength region have been recently the subject of intensive research, because of their strong potential for creating novel device structures with high performance. Three-dimensional periodic dielectric structures (so-called photonic crystals or photonic lattices) can display complete photonic bandgaps, as first described by Yablonovitch [13] and John [14]. However, in practice, 2-D photonic lattice struc-

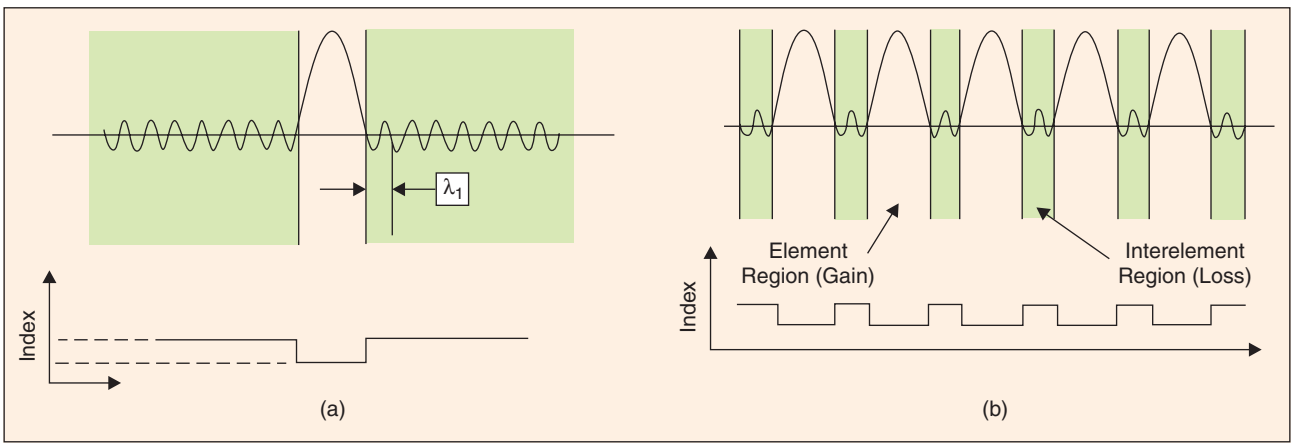

1. (a) Schematic diagram of single antiguide. (b) Schematic diagram of antiguided array structure.

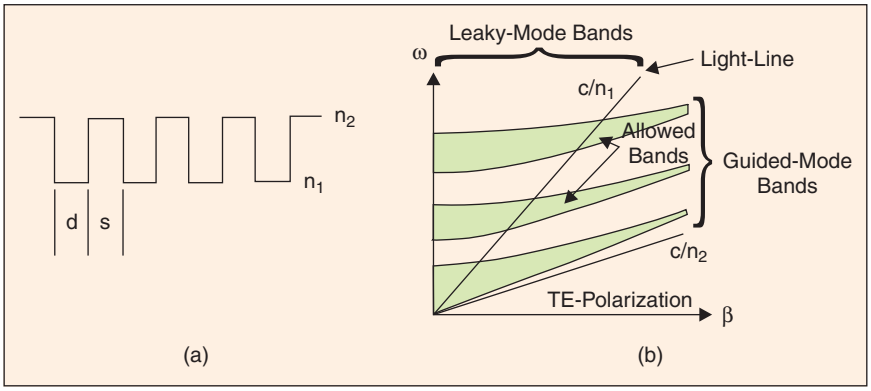

2. (a) One-dimensional periodic index profile representing an array structure. (b) Schematic representation of the dispersion diagram illustrating the regions of guided-mode bands and leaky-mode bands.

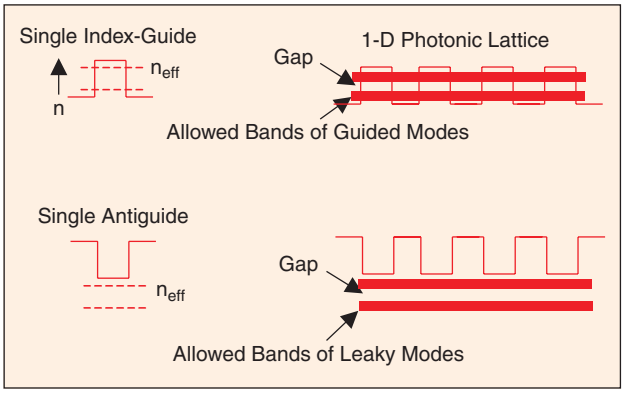

3. (a) Single waveguide guided modes and formation of guided-mode bands in an array structure. (b) Single antiguided modes and formation of leaky-mode bands in an array structure.

tures are considerably easier to fabricate and also can exhibit a photonic bandgap in the plane of the lattice [15], [16]. These structures can be classified into either *passive* photonic lattices, with applications such as angular independent high-reflectivity mirrors [17] and low-loss defect-waveguides [18], or *active* photonic lattices, such as microcavity-defect lasers [19], 2-D distributed feedback-type lasers [20], 1-D antiguided phase-locked laser arrays [7], and 2-D VCSEL phase- locked arrays [21].

A common attribute shared by photonic-lattice-based devices, with the notable exception of antiguided-array structures [7], [8], [10], is that they are designed to operate *within* the photonic bands bounded by the *light line* (representing photon propagation in the low-index material) [16]. A schematic dispersion diagram for a 1-D photonic lattice is shown in Figure 2, indicating the allowed bands for guided and leaky modes. For an infinite 1-D periodic dielectric structure, Bloch function analysis can be used to determine the propagating Bloch-wave solutions [22]. Bands of propagating solutions are separated by forbidden gaps, corresponding to evanescently decaying solutions. The group of allowed bands below the light line are called the guided-mode bands. This terminology stems from the fact that the bands can be considered to originate from the guided modes of "high-index" waveguides, as shown schematically in Figure 3(a). For example, photonic-lattice structures such as coupled VCSEL arrays [21] confine light to the allowed optical modes within the guided-mode bands. Laser oscillation has also been reported from 2-D distributed feedback type structures constructed using organic or polymer gain materials [20] as well as semiconductor materials [23]. These 2-D photonic lattices consist of a gain medium with periodic air holes forming either a triangular or square lattice geometry. Laser action occurs in the guided-mode bands of the photonic lattice, since gain is supplied only in the high-index regions of the lattice.

In contrast, structures such as antiguided arrays act to confine light within the allowed photon modes corresponding to the *leaky-mode bands* of the photonic lattice [i.e., above the light line (see Figure 2)], *as long as* there is enough gain to compensate for radiation losses. The leaky-mode bands originate from the modes confined to the high-gain, low-index regions (antiguides) of the lattice [Figure 3(b)]. The Bloch-function formalism has been shown to be useful for analyzing the leaky modes of both infinite [24] as well as finite 1-D antiguided array structures [25]. The calculated photonic band structure, using Bloch-function analysis, for an infinite 1-D lattice is shown in Figure 4(a). The allowed leaky-mode solution bands lie below the low index of the structure (n=3.3) and are separated by forbidden gaps (dark regions). The leaky modes for the finite array structure have been shown to fall within the allowed bands of the infinite structure, as shown in Figure 4(b) for selected finite array modes [25]. The resonant modes correspond to regions where the band edges cross (i.e., no forbidden gap), and this occurs when the interelement width becomes equal to an integer number of half-lateral wavelengths. As active structures, 1-D antiguided arrays have also been theoretically investigated above lasing threshold [26], allowing an understanding of the modal behavior in the presence of nonlinear gain effects. However, the leaky-mode photonic band structure of 2-D antiguided structures has been largely unexplored. Furthermore, a comprehensive theoretical analysis of the leaky-mode behavior *above* laser threshold is needed to optimize such structures for stable, single-mode operation. Nonlinear effects such as gain-spatial-hole burning (GSHB) and self-focusing and defocusing of the optical mode under carrier- and thermally induced index variation need to be considered to understand the modal behavior of actual devices above laser threshold.

Photonic-lattice-based microcavity laser structures localize light to a defect mode generally within a forbidden gap lying between the guided-mode bands [19]. This type of localized mode can exhibit a high cavity Q and a small modal volume, making the structure ideal for the waveguide of a microcavity laser. Villeneuve et al. and Krauss et al. demonstrated the possibility of

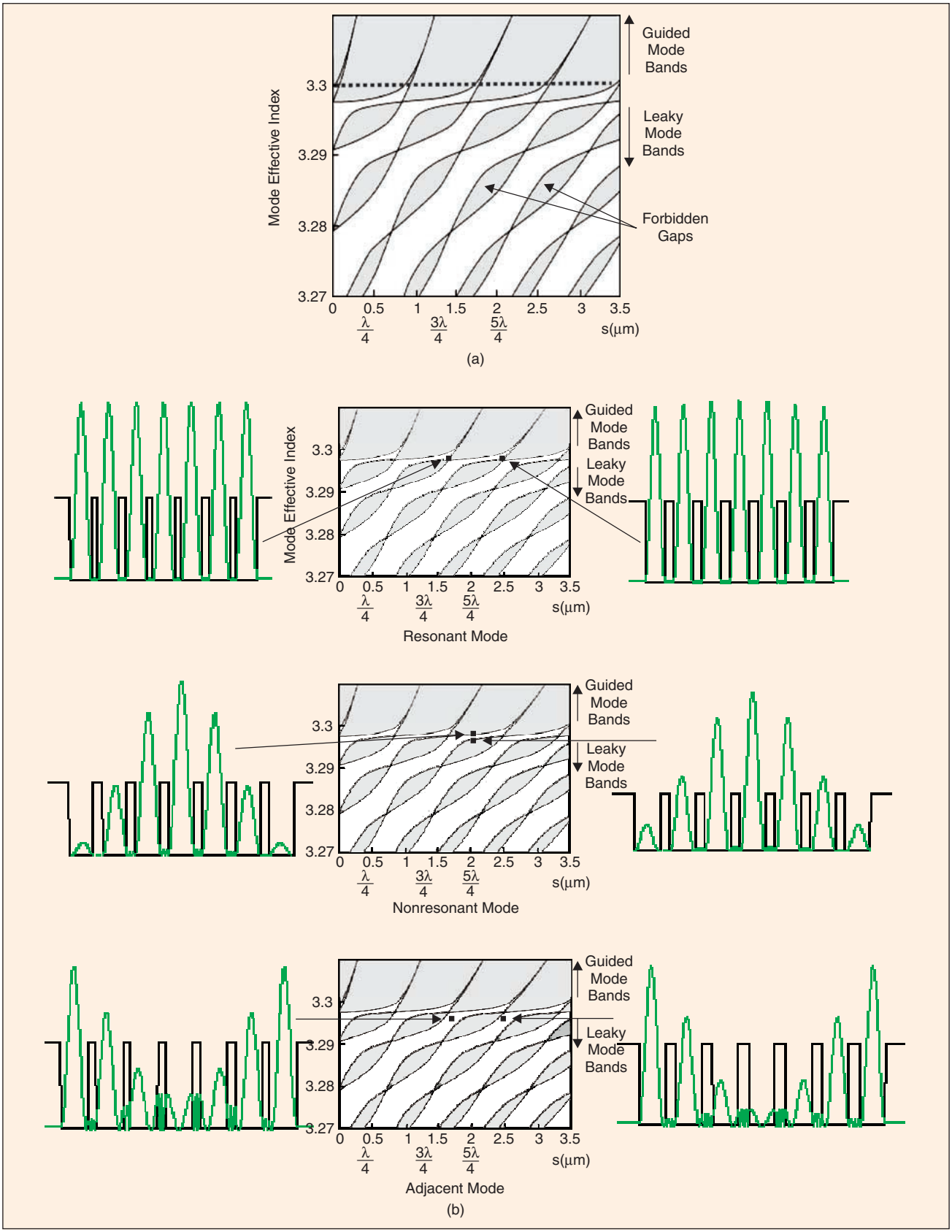

4 (a) Calculated photonic band diagram (i.e., modal index versus high-index spacing) for an infinite 1-D array structure. Allowed leaky-mode solution bands (below 3.3 index) are separated by forbidden gaps (dark regions). (b) Calculated finite array modes and positions within the allowed infinite bands for resonant in-phase, nonresonant in-phase, and adjacent modes.

forming defect states in the forbidden gaps between leaky-mode bands [16], [27]. Such photon states are less localized than the guided-mode defect states and, due to radiation losses, exhibit a lower cavity Q. Although the transmission characteristics of photonic lattices with a leaky-mode defect were analyzed [27], active devices have not been investigated. The existence of localized defect states above the light line (i.e., in the gaps between leaky-mode bands) may allow for the possibility to fabricate novel active structures with properties *dependent* on the supporting photonic lattice. These types of leaky-mode defect structures are currently being studied in the form of ARROW-type VCSELs [28].

2-D VCSEL Array Structures

The coupled-lasing modes of the VCSEL array represent the allowed bands of propagating Bloch waves in the 2-D active photonic lattice. Previous VCSEL array designs have attempted to select a single mode (i.e., all elements phase-locked) from the allowed bands of *guided-modes* of the 2-D photonic lattice. However, stable, high-power, diffraction-limited beam operation from 2-D VCSEL arrays has not been realized [21], [29], [30]. All previously reported phase-locked 2-D VCSEL arrays operate in either out-of-phase mode or a mixture of various modes, characteristic of weakly index-guided arrays, with poor intermodal discrimination. To achieve in-phase-like emission characteristics, external phase-shifters have also been used on optically pumped VCSEL arrays [31]; however, the resulting beam is quite broad. The progress in phase-locked 2-D VCSEL arrays parallels closely that of edge-emitting phase-locked arrays. Weak coupling and poor intermodal discrimination found in evanescently coupled edge-emitting laser arrays have severely limited their single-mode output power due to gain spatial hole burning at the array level [32].

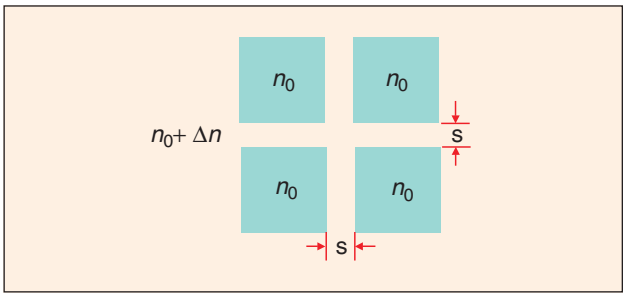

5. Effective-index modeling structure for 2×2 array with Δn=0.05 and d=6 μm: s represents the interelement spacing and n_0 is the effective index of the element region

In contrast to positive-index-guided VCSEL arrays, antiguided VCSEL arrays operate in the allowed leaky-mode bands of the 2-D photonic lattice. As a result, the antiguided array structure exhibits strong leaky-wave coupling leading to high intermodal discrimination [7]. The large built-in index step and strong lateral radiation leakage from antiguides make them well suited for array integration. Serkland et al. [33] has recently demonstrated leaky-wave coupling between two antiguided VCSELs (coupled in-phase or out-of-phase) using structures fabricated with a cavity-induced resonance shift. We have recently demonstrated that 2-D (4×4) 16-element VCSEL arrays can be designed to operate in a stable in-phase mode in good agreement with theory [34], [35]. Since the VCSEL elements are coupled by traveling-wave radiation, resonant coupling [34], [35] for the in-phase (out-of-phase) mode occurs when the interelement spacing corresponds to an odd (even) integral number of half-waves of the antiguide radiation leakage.

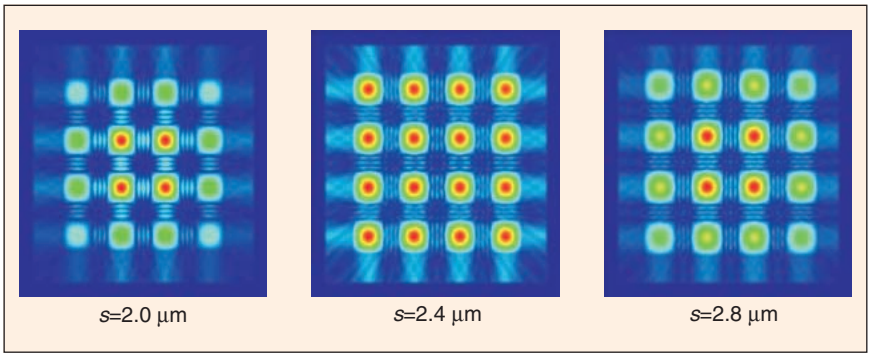

6. Calculated near-field intensity profiles for the in-phase mode as a function of low-index (element) spacing s. At s=2.4 μm, the structure is laterally resonant.

For a single antiguide with a core index of n_0 and index step of $\Delta n=n_1-n_0$, the antiguided fundamental mode exhibits a radiating field into the high-index cladding regions characterized by a lateral wavelength λ_1 that can be approximated by [7]

$$\lambda_1 = \lambda_0 \Big/ \left(n_1^2 - n_0^2 + \lambda_0^2/4d^2\right)^{1/2} \tag{1}$$

where λ_0 is the vacuum wavelength and d is the low-index "core" width.

In a 1-D antiguided array, each element has radiation loss into the neighboring high-index regions with a lateral wavelength λ_1 also approximated by (1). The lateral traveling waves within the structure couple all elements together and form vari-

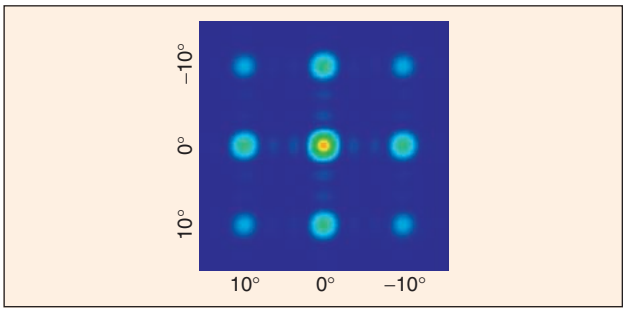

7. Calculated far-field pattern for a 4×4 array operating in an in-phase mode.

ous array modes: in-phase modes, out-of-phase modes, and adjacent modes (neither in-phase nor out-of-phase; i.e., varying phase between elements). When the array interelement spacing s satisfies the resonant condition, that is

> Photonic-lattice structures in the near-IR wavelength region have been recently the subject of intensive research, because of their strong potential for creating novel device structures with high performance.

$$s = m\lambda_1/2 \tag{2}$$

where m is an integer number, the array exhibits resonant coupling (even values of m correspond to the out-of-phase mode resonance and odd values corresponds to the in-phase resonance). As a result, the resonant modes have uniform near-field profile across the array and negligible interelement field. While we expect similar values of s for resonance in the 2-D array structure, there may be some differences as a result of the 2-D coupling.

Due to the difficulties in studying a complete 3-D multilayer structure, we utilize the effective-index model and fiber-mode approximation to calculate the modal behavior of the 2-D VCSEL array structure [34], [35]. In this approximation, the array elements and outer regions are simply represented by the effective indices n_0 and n_1, respectively, calculated from the 1-D transverse layered structure in each region. The 3-D structure is then transferred into a 2-D "fiber array." For simplicity, we studied the leaky-mode behavior of a 4×4 antiguided VCSEL array, a truncated version of which is shown in Figure 5. The 16 square regions represent the array elements that have effective indices (n_0) lower than that (n_1) in the inter-element and background regions. In this calculation, the element width d=6 μm and index step Δn=0.05 (n_0=3.3, n_1=3.35). From (1), the lateral wavelength of this design at vacuum wavelength λ_0=980 nm is λ_1=1.68 μm. From (2), the out-of-phase and in-phase mode resonance occurs for interelement width s=λ_1(1.68 μm) and 1.5 λ_1 (2.5 μm), respectively.

As described previously [35], we define the 2-D array mode as mode (m,n) where m is the number of standing wave nulls in the horizontal direction and n is the number of nulls in the vertical direction. Therefore, for a 4×4 array, mode (9,9) is an out-phase mode, mode (12, 12) is an in-phase mode (corresponds to 3-half lateral waves), and mode (12, 14) is an adjacent mode. The calculated in-phase mode (12,12) is shown in Figure 6, as a function of interelement spacing (i.e., high-index region width). Starting from s=2.0 μm, the in-phase mode (12, 12) has a very nonuniform (cosine shape) near field, characteristic of nonresonant modes. At s=2.4 μm (~$3\lambda_1/2$), the mode exhibits a nearly uniform near-field profile, characteristic of the lateral resonance. As s increases to 2.8 μm, the field becomes more like a cosine-shaped profile again. The nonuniform field profile of the nonresonant mode is vulnerable to GSHB and thermal lensing, leading to multimode operation. Therefore, it is desirable to design the structure to operate in the resonant mode.

The calculated far-field intensity profile for an array operating in the in-phase mode is shown in Figure 7. A central on-axis lobe occurs with side lobes, which are dependent on the array fill factor. Because of the square symmetry of the lattice, the in-phase mode always has the main power in the center lobe with surrounding smaller lobes forming a square pattern, and the out-of-phase mode has its power divided into four primary lobes.

Because of the desirable far-field pattern, we would like to design the 2-D array to operate in the resonant in-phase mode. Therefore, it is important to understand the mode selection mechanisms in the antiguided structure. There are three primary mechanisms that result in mode selectivity: 1) lateral edge radiation losses, 2) 2-D modal overlap with the active layer gain, and 3) modal absorption losses due to placing lossy layers within the structure (typically in the interelement, high-index regions). In antiguided VCSEL arrays, the 2-D modal gain overlap is similar for all supported modes in a uniformly pumped device, so this plays a small role in mode selection. Calculations indicate that the combination of lateral radiation losses, which are highly mode dependent, and interlement losses result in a design space allowing the resonant in-phase mode to oscillate. This is because losses placed in the interelement regions of the array selectively af-

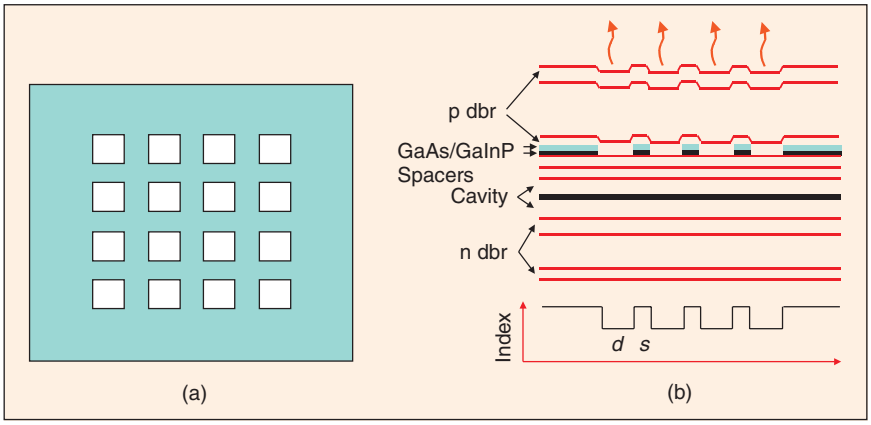

8. (a) Top view and (b) cross-section view of the 4×4 antiguided VCSEL arrays: d is the element (low-index) width and s is the interelement (high-index) spacing.

fect the nonresonant modes, which have relatively large field intensity in the high-index regions of the array.

Top-emitting antiguided array structures (d=6 μm, Δn=0.05) were fabricated using a two-step MOCVD growth process [34] and selective wet chemical etch. It consists of 32.5 pairs of AlAs/ GaAs n-DBR, 23 pairs of $Al_{0.15}GaAs$/GaAs p-DBR, and 1-λ optical cavity that includes 3-InGaAs quantum wells, GaAs barrier layers, and $Al_{0.3}GaAs$ confinement layers for 980 nm emissions. The first growth consists of n-DBR, cavity, one pair of p-DBR, and two thin spacer layers of GaAs (10 nm) and GaInP (12 nm). The purpose of these thin layers is to generate an effective index step between the interelement and element regions. The calculated effective index step for this structure is Δn=0.05. A schematic cross section of the 2-D array structure is shown in Figure 8.

We use H_3PO_4:H_2O_2:H_2O (1:1:5) and HCl:H_2O (4:1) to selectively etch away the GaAs and GaInP thin layers under the emitting elements area and then regrow the remaining top p-DBR. Following processes include defining the current aperture by H^+ ion implantation, making top and bottom ohmic contacts, as well as opening the optical window. The interelement (high-index region) width s was adjusted between 2 and 3.5 μm to select either the in-phase or out-of-phase resonance condition. Note that in these initial structures we do not intentionally include absorbing layers for interelement loss to aid the suppression of nonresonant modes, as discussed above. It's noteworthy to point out that, because the metal contact on top of the high-index regions (as shown in Figure 8) introduces additional losses for the guided-array modes, we expect the array to operate only in the leaky modes even though the array is uniformly pumped. In fact, these metal losses may also be effective in suppressing nonresonant leaky modes.

> In contrast to positive-index-guided VCSEL arrays, antiguided VCSEL arrays operate in the allowed leaky-mode bands of the 2-D photonic lattice.

CW single-mode in-phase emission is observed from arrays with interelement widths of s=2.5 μm with the characteristics of an on-axis-lobe far-field pattern. At s=3.0 μm, single out-of-phase mode operation with the resulting four-lobe far-field pattern is obtained. The measured CW far-field emission pattern for an array with s=2.5 μm (in-phase), as captured by a CCD camera, is shown near laser threshold in Figure 9. The angular lobe separation and widths are obtained from the 1-D scan of the far-field intensity for the arrays with the full-width half-maximum (FWHM) for the in-phase mode of about 2^o, and the side lobes separation of 13.5^o, in agreement with the calculation. The emission patterns remain stable up to the maximum thermally limited CW output power (~1-2 mW) and pulsed output power greater than 40 mW (Figure 10).

Future Optimization and Conclusions

By placing gain in the low-index lattice sites of the 2-D antiguided VCSEL array we can excite the leaky modes and exploit the unique properties of this 2-D active photonic lattice. As a result, large aperture sources with high spatial coherence can be achieved. Numerical simulation indicates scaling to over 100 elements can be achieved, while maintaining single-mode emission. Recently, we have fabricated 2-D VCSEL arrays as large as 20 × 20 (i.e., 400 elements), which demonstrate in-phase mode operation. However, strong heating in these devices will require junction-down heatsinking with substrate side emission to avoid thermal lensing problems.

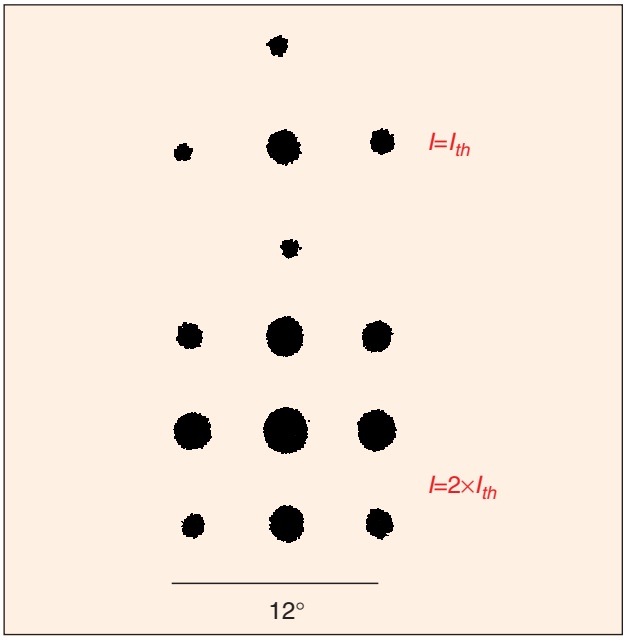

9. Measured CW far-field patterns for a 4×4 array operating in the in-phase mode, showing good agreement with theory (Figure 7).

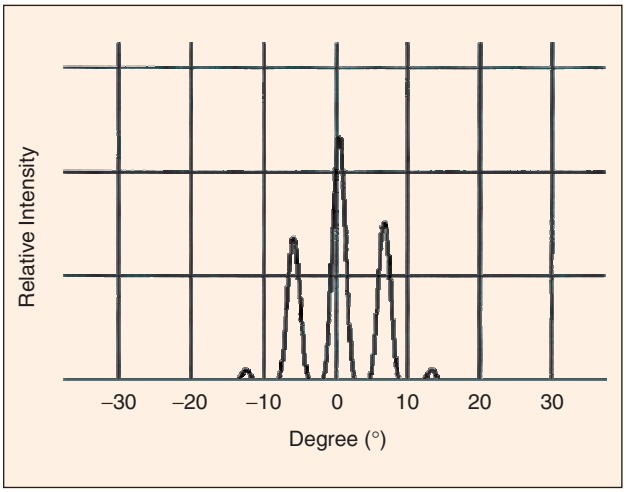

10. Measured 1-D scan of the in-phase mode's far-field distribution at 40 mW pulsed output power.

Acknowledgments

Delai Zhou, Ling Bao, Nam Kim, N.N. Elkin, and A.P. Napartovich have made technical contributions to the work described in this manuscript. NSF provided funding under Grant No. 0139823.

Luke J. Mawst is with the Reed Center for Photonics and Department of Electrical Computer Engineering at the University of Wisconsin-Madison, Wisconsin, USA. E-mail: mawst@engr.wisc.edu.

References

[1] K.D. Choquette, H.Q. Hou, G.R. Hadley, and K.M. Geib, "High power single transverse mode selectively oxidized VCSELs," presented at 1997 Summer Top. Meet. on Vertical-Cavity Lasers, Montreal, Quebec, Canada, Aug. 1997.

[2] C. Jung, R. Jager, M. Grabherr. P. Schnitzer, R. Michalzik, B. Weigl, S. Muller, and K. Jebeling, "4.8 mW single mode oxide confined top-surface emitting vertical-cavity laser diodes," *Electron Lett.,* vol. 33, p. 1790, 1997.

[3] D. Botez, "Monolithic phase-locked semiconductor laser arrays," in *Diode Laser Arrays*, D. Botez and D.R. Scifres, Eds. Cambridge, UK: Cambridge Univ. Press, 1994, pp. 1-72.

[4] Y.A. Wu, G.S. Li, R.F. Nabiev, K.D. Choquette, C. Caneau, and C.J. Chang-Hasnain, "Single-mode, passive antiguide vertical cavity surface emitting laser," *IEEE J. Selected Topics Quantum Electron*., vol. 1, p. 629, June 1995.

[5] T.H. Oh, M.R. McDaniel, D.L. Huffaker, and D.G. Deppe, "Cavity-induced antiguiding in a selectively oxidized vertical-cavity surface-emitting laser," *IEEE Photon Tech. Lett.*, vol. 10, p. 12, Jan. 1998.

[6] K.D. Choquette, G.R. Hadley, H.Q. Hou, K.M. Geib and B.E. Hammons, **"**Leaky mode vertical cavity lasers using cavity resonance modification," *Electron. Lett.,* vol. 34, p. 991, 1998.

[7] D. Botez, L.J. Mawst, G. Peterson, and T.J. Roth, "Phase-locked arrays of antiguides: Modal content and discrimination," *IEEE J. Quantum Electron.*, vol. 26, pp. 482-495, March 1990.

[8] D. Botez, M. Jansen, L.J. Mawst, G. Peterson, and T.J. Roth, "Watt-range, coherent, uniphase power from phase-locked arrays of antiguide diode lasers," *Appl. Phys. Lett.*, vol. 58, pp. 2070-2072, May 1991.

[9] L.J. Mawst, D. Botez, C. Zmudzinski, and C. Tu, "Design optimization of ARROW-type diode lasers," *IEEE Photonics Tech. Lett*., vol. 4, pp. 1204-1206, Nov. 1992.

[10] H. Yang, L.J. Mawst, M. Nesnidal, J. Lopez, A. Bhattacharya, and D. Botez, "10 W near-diffraction-limited pulsed power from 0.98 μm-emitting, Al-free phase-locked antiguided arrays," *Electron Lett.,* vol. 33, pp. 136-138, 1997.

[11] G.R. Hadley, "Effective index model for vertical-cavity surface-emitting lasers," *Opt. Lett.*, vol. 20, p. 1483, 1995.

[12] R.W. Engelmann and D. Kerps, "Leaky modes in active three-layer slab waveguides," *Proc. Inst. Electr. Eng. I, Solid State and Electron. Devices*, vol. 127, p. 330, 1980.

[13] E. Yablonovitch, "Inhibited spontaneous emission in solid-state physics and electronics," *Phys. Rev. Lett.*, vol. 58, p. 2059, 1987.

[14] S. John, "Strong localization of photons in certain disordered dielectric superlattices," *Phys. Rev. Lett.*, vol. 58, p. 2486, 1987.

[15] H. Benisty, C. Weisbuch, D. Labilloy, M. Rattier, C.J.M. Smith, T.F. Krauss, R.M. De La Rue, R. Houdre, U. Oesterle, C. Jouanin, and D. Cassagne, "Optical and confinement properties of two-dimensional photonic crystals," *J. Lightwave Tech*., vol. 17**,** p. 2063, 1999.

[16] P.R. Villeneuve, S. Fan, S.G. Johnson, J.D. Joannopoulos, "Three-dimensional photon confinement in photonic crystals of low-dimensional periodicity," *Proc. Inst. Electr. Eng. - Optoelectron*., vol. 145, p. 384, 1998.

[17] M. Rattier, H. Benisty, C.J.M. Smith, A. Beraud, D. Cassagne, C. Jouanin, T.F. Krauss, and C. Weisbuch, "Performance of waveguide-based two-dimensional photonic-crystal mirrors studied with Fabry-Perot resonators," *IEEE J. Quant. Electron.*, vol. 37, p. 237, 2001.

[18] A. Adibi, Y. Xu, R.K. Lee, A. Yariv, A. Scherer, "Properties of the slab modes in photonic crystal optical waveguides," *J. Lightwave Technol.*, vol. 18, p. 1554, 2000.

[19] O.J. Painter, A. Husain, A. Scherer, J.D. O'Brien, I. Kim, P.D. Dapkus, "Room temperature photonic crystal defect laser at near-infrared wavelengths in InGaAsP," *J. Lightwave Technol.*, vol. 17, p. 2082, 1999.

[20] M. Meier, A. Mekis, A. Dodabalapur, A. Timko, R.E. Slusher, J.D. Joannopoulos, O. Nalamasu, "Laser action from two-dimensional distributed feedback in photonic crystals," *Appl. Phys. Lett*., vol. 74, p. 7, 1999.

[21] R.A. Morgan, K. Kojima, T. Mullally, G.D. Guth, M.W. Focht, R.E. Leibenguth, and M. Asom, "High-power coherently coupled 8x8 vertical cavity surface emitting laser array," *Appl. Phys. Lett*. vol. 61, p. 1160, 1992.

[22] P. Yeh, *Optical Waves in Layered Media*. New York: Wiley, 1988.

[23] M Imada, S. Noda, A. Chutinan, T. Tokuda, M. Murata, and G. Sasaki, "Coherent two-dimensional lasing action in surface-emitting laser with triangular-lattice photonic crystal structure," *Appl. Phys. Lett*., vol. 75, p. 316, 1999.

[24] R. Nabiev and A.I. Onishchenko, "Laterally coupled periodic semiconductor laser structures: Bloch function analysis," *IEEE J. Quantum Electron*, vol. 28, pp. 2024-2032, Oct. 1992.

[25] C.A. Zmudzinski, D. Botez, and L.J. Mawst, "Simple description of laterally resonant, distributed-feedback-like modes of arrays of antiguides," *Appl. Phys. Lett.,* vol. 60, pp. 1049-1051, 1992.

[26] R.F. Nabiev and D. Botez, "Comprehensive above-threshold analysis of antiguided diode laser arrays," *IEEE J. Selected Topics Quantum Electron.*, vol. 1, pp. 138-149, 1995.

[27] T.F. Krauss, B. Vogele, C.R. Stanley, R.M. De La Rue, "Waveguide microcavity based on photonic microstructures," *IEEE Photon. Tech. Lett*., vol. 9, p. 176, 1997.

[28] D. Zhou and L.J. Mawst, "Simplified-antiresonant reflecting optical waveguide-type vertical-cavity surface-emitting lasers," *Appl. Phys. Lett*., vol. 76, p. 1659, 2000.

[29] J.P. Van Der Ziel, D.G. Deppe, N. Chand, G.J. Zydzik, and S.N.G. Chu, "Characteristics of single- and two-dimensional phase couples arrays of vertical cavity surface emitting GaAs-AlGaAs lasers," *J. Quantum Electron*., vol. 26, p. 1873, 1990.

[30] M. Orenstein, E. Kapon, N.G. Stoffel, J.P. Harbison, L.T. Florez, and J. Wullert, "Two-dimensional phase-locked arrays of vertical-cavity semiconductor lasers by mirror reflectivity modulation," *Appl. Phys. Lett*., vol. 58, p. 804, 1991.

[31] M.E. Warren, P.L. Gourley, G.R. Hadley, G.A. Vawter, T.M. Brennan, B.E. Hammons, and K.L. Lear, "On-axis far-field emission from two-dimensional phase-locked vertical cavity surface-emitting laser arrays with an integrated phase-corrector," *Appl. Phys. Lett*., vol. 61, p. 1484, 1992.

[32] K-L. Chen and Shyh Wang, "Spatial hole burning problems in evanescently coupled semiconductor laser arrays," *Appl. Phys. Lett.,* vol. 47, p. 555, 1985.

[33] D.K. Serkland, K.D. Choquette, G.R. Hadley, K.M. Geib, and A.A. Allerman, "Two-element phased array of antiguided vertical-cavity lasers," *Appl. Phys. Lett*., vol. 75, p. 3754, 1999.

[34] D. Zhou and L.J. Mawst, "Two-dimensional phase-locked antiguided vertical-cavity surface-emitting laser arrays," *Appl. Phys. Lett*., vol. 77, p. 2307, 2000.

[35] D. Zhou and L.J. Mawst, "Modal properties of two-dimensional antiguided vertical-cavity surface-emitting laser arrays," *IEEE J. Quantum Electron.*, vol. 38, p. 652, June 2002. CD■